MAGNETIC PROPERTIES OF $Dy_2Ti_2O_7$

/

by D. J. Flood
Lewis Research Center
Cleveland, Ohio 44135

MAGNETIC PROPERTIES OF $Dy_2Ti_2O_7$

by D. J. Flood

Lewis Research Center
National Aeronautics and Space Administration
Cleveland, Ohio

ABSTRACT

Measurements have been made of the magnetization, differential magnetic susceptibility, and magnetic entropy of powdered samples of $Dy_2Ti_2O_7$. The saturation magnetic moment is 4.7±0.2 Bohr magnetons per Dy ion, instead of 10 as predicted by Hund's rules. A temperature-independent magnetization is observed in the saturation region. Absolute values of magnetic entropy have been obtained for temperatures from 1.25 to 20 K, in applied fields up to 10.4 tesla. The magnetic entropy approaches a maximum value consistent with a ground-state multiplicity of 2. Low field magnetization and differential susceptibility data show a transition to antiferromagnetism near 1.35 K. A construction of the magnetic specific heat from the zero field entropy shows an anomaly near the same temperature.

INTRODUCTION

$Dy_2Ti_2O_7$ is one of a group of cubic compounds with the formula $R_2M_2O_7$, where R is a rare-earth, and M is one of the metals Ti, Sn, or Zn. The compounds have a crystal structure very similar to that of the mineral pyrochlore (ref. 1). Extensive studies of $Er_2Ti_2O_7$ have been made (ref. 2) and show that at least for the Ti compounds the rare-earth ions are located at sites of trigonal symmetry, with each one surrounded by 8 oxygen ions. The f.c.c. unit cell contains 16 rare-earth ions, arranged such that any one of them has 6 other rare-earth ions at equal distances from it. Figure 1 (from ref. 1) shows a schematic representation of the details discussed above.

EXPERIMENTAL METHODS

The compound was obtained from a commercial supplier in powder form. A portion of the sample was tightly packed into one of two hollow phenolic cylinders which were wound with nearly identical 750 turn pick-up coils. The pick-up coils were connected in series opposition to one another, and the difference voltage was applied to the input of an integrator. This arrangement automatically eliminated the large background emf caused by the changing magnetic field itself. The measurements were made by suspending the cylinders side-by-side in a helium bath at the center of a 10 centimeter (4") diameter bore, water-cooled solenoid capable of producing magnetic fields in excess of 7 tesla. A schematic diagram of the experiment is shown in figure 2. The sample was 0.8 cm in diameter and 5.2 cm in length with a density of 3.86 gm/cm^3.

The differential susceptibility was measured by superimposing a small oscillating magnetic field on the sample and detecting the induced emf with a lock-in amplifier. The output of the lock-in amplifier, which was proportional to dM/dH, was plotted either as a function of temperature for fixed magnetic field, or as a function of magnetic field at constant temperature.

Magnetic entropy measurements were made on a sample closely shaped to the form of an ellipsoid of revolution (semi-major axis 1.02 cm, semi-minor axis 0.413 cm). A portion of the powder was sintered into a solid rod with a density of 5 gm/cm^3, and the ellipsoidal sample was ground from one section. Figure 3 illustrates how the magnetic entropy of the compound was measured. A heater was non-inductively wound on the sample, which was suspended in a vacuum can, and connected to a temperature controller. The sensing element for the controller was a glass-ceramic capacitor (ref. 3) that was glued to a thin copper strip. The copper strip was wrapped around the sample so that its ends did not quite touch, and glued securely in place. Two voltages, one proportional to the heater current, and the other to the heater voltage, were used as inputs to an electronic multiplier. The output of the multiplier, which was proportional to the power supplied to the heater, was in turn used as the input to an integrator. The integrator output, proportional to the heat produced by the heater, was plotted as a function of magnetic field on an X-Y plotter.

Measurements were made of the amount of heat required to keep the sample at a constant temperature as the magnetic field was reduced. A 10.4 tesla, 6.25 cm (2.5 in.) diameter bore superconducting solenoid was used for these measurements in addition to the magnet mentioned earlier. The superconducting magnet possessed a remnant field of approximately 0.35 tesla. In order to record the total entropy change available, it was necessary to use the water-cooled solenoid for the field range from 0 to 5 tesla. Overlapping sets of data from 1T to 5T were taken to check the reproducibility of the measurements.

RESULTS AND DISCUSSION

Figure 4 shows the magnetization as a function of applied magnetic field for three different temperatures in the liquid helium range. The saturation region has superimposed on it a linear magnetization whose slope is independent of temperature. A contribution of this sort to the magnetization is an indication that some mixing of the ground state wave function with the wave function for an upper level has occurred (ref. 4). The resulting perturbation of the system produces a non-zero off-diagonal matrix element of the magnetic moment operator. The slope of the linear contribution is a measure of the magnitude of the matrix element, but an estimate of the separation of the levels is needed in order to make the calculation.

Extrapolation of the linear portion at saturation to zero field yields a value for M_s of $(3.79 \pm 0.08) \times 10^5$ ampere-turns/meter. Inserting this value in the expression for the saturation magnetization, which is

$$M_s = N\mu_B g J \tag{1}$$

yields $gJ = 4.7 \pm 0.2$ for the effective number of Bohr magnetons per ion. (μ_B is the Bohr magneton, g the spectroscopic splitting factor, and J is the total angular momentum quantum number.) $N = 8.7 \times 10^{21}$ ions/cm^3 for the sample used in the measurements. The free-ion value predicted by Hund's rules is 10. The large discrepancy indicates that crystal field effects have drastically perturbed the ground state of the Dy ions. It is interesting

to note that low-field susceptibility measurements do not necessarily indicate any such discrepancy. In the low field case, the effective number of Bohr magnetons per ion is, from the Curie-Weiss law,

$$p_{eff} = g\sqrt{J(J+1)} = \frac{3Ck_B}{N\mu_B^2} \tag{2}$$

where C is the Curie constant and k_B is the Boltzmann constant. In this case Hund's rules predict a value of 10.63. van Geuns (ref. 5) measured the susceptibility of spherical samples formed by sintering $Dy_2Ti_2O_7$ powder into a solid, and found $p_{eff} \simeq 10$. Figure 5 contains a plot of $1/\chi$ as a function of temperature, where χ was determined from the initial slopes of the magnetization curves. Although magnetic interactions are becoming important as the Néel temperature is approached, so that deviations from the Curie-Weiss law are expected, nonetheless, even these data indicate that $p_{eff} = 9.6 \pm 0.3$. The problem is to properly take into account the effects of crystalline anisotropy in a powdered material.

The transition to the antiferromagnetic state which is indicated by the data in figure 5 is shown with more precision in figure 6. Here is shown the inverse of the differential magnetic susceptibility as a function of temperature. The temperature at which $1/\chi_{diff}$ is a minimum is in good agreement with that reported by Cashion, et al. (ref. 6) from measurements on single crystals of $Dy_2Ti_2O_7$.

The magnetic entropy of the compound is shown in figure 7 as a function of magnetic field at several temperatures. The close approach to zero entropy at the lower temperatures and high fields is clearly evident. The higher temperature isotherms, for which the zero entropy could not be reached by 10.4 T, were positioned in the S-H plane by adiabatically magnetizing and demagnetizing from a temperature for which the absolute value of the magnetic entropy was known. The lattice entropy was assumed to be

$$s_l = \frac{1}{3}aT^3 \tag{3}$$

where $a = 2.2 \times 10^{-6}$ joules/gm$^\circ$K is the lattice specific heat constant reported by van Geuns (ref. 2).

Figure 8 shows a construction of the entropy-temperature plane from data such as are shown in figure 7. The entropy approaches a maximum value which is consistent with a ground-state multiplicity of 2 rather than 16, as would be the case if the ions were not perturbed by crystalline field interactions.

The zero-field plot of magnetic entropy may be used to calculate the magnetic specific heat of the compounds, since

$$C = T \frac{\Delta S}{\Delta T} \tag{4}$$

The resulting plot of C as a function of temperature is shown in figure 9. In this particular case the results are not very precise. They are presented to show only that such information can be obtained, and that the thermal measurements are in accord with the magnetic measurements discussed above.

SUMMARY

Saturation magnetization measurements on powdered samples of $Dy_2Ti_2O_7$ yield a value of 4.7 ± 0.2 Bohr magnetons per Dy ion. Low-field susceptibility data, which appear to fit a Curie-Weiss law, give a value of 9.6 ± 0.3 Bohr magnetons per ion, which is more nearly consistent with the Hund's rules' prediction of 10.6 μ_B. The discrepancy apparently arises because of strongly anisotropic crystalline field effects, since magnetic entropy data indicate that the ground state has a multiplicity of 2, rather than 16. Measurements of several isotherms in the magnetic entropy-magnetic field plane have been used to construct the iso-field lines in the magnetic entropy-temperature plane. Anomalies in the susceptibility and magnetic specific heat indicate a transition to the antiferromagnetic state near 1.35 K, in agreement with other work (ref. 5).

REFERENCES

1. H. W. J. Blote, R. F. Wielinga, and W. J. Huiskamp, Physica 43, 549 (1969).

2. O. Knop, F. Brisse, L. Castelliz, and Sutarno, Can. J. Chem. 43, 2812 (1965).

3. W. N. Lawless, Rev. Sci. Instr. 42, 561 (1971).

4. J. H. van Vleck, The Theory of Electric and Magnetic Susceptibility (Oxford Univ. Press, London, 1932).

5. J. R. van Geuns, "A Study of a New Magnetic Refrigeration Cycle," Thesis, University of Leiden, (1966).

6. J. D. Cashion, A. H. Cook, M. J. M. Leask, T. L. Thorp, and M. R. Wells, J. Mat. Sci. 3, 395 (1968).
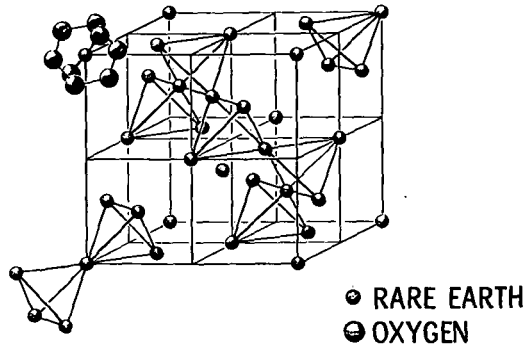
Figure 1. - Crystal structure of $Er_2Ti_2O_7$. The f.c.c. unit cell contains 8 $Er_2Ti_2O_7$ groups.

● RARE EARTH
● OXYGEN
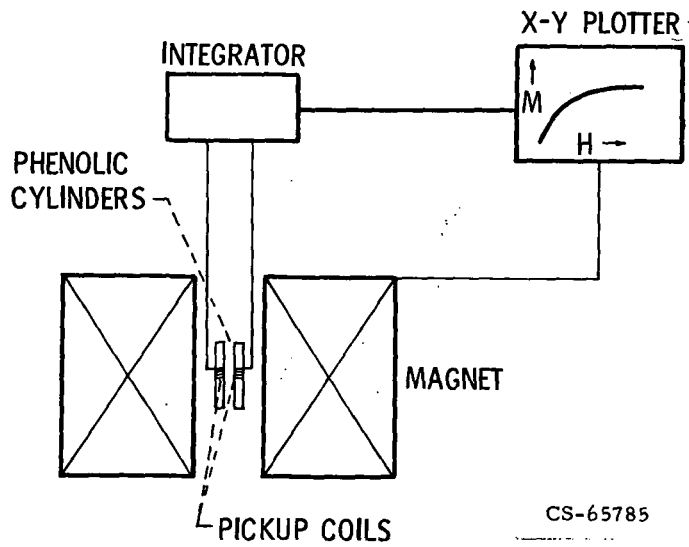
CS-65780

Figure 2. - Schematic diagram of magnetization measurement technique.

CS-65785
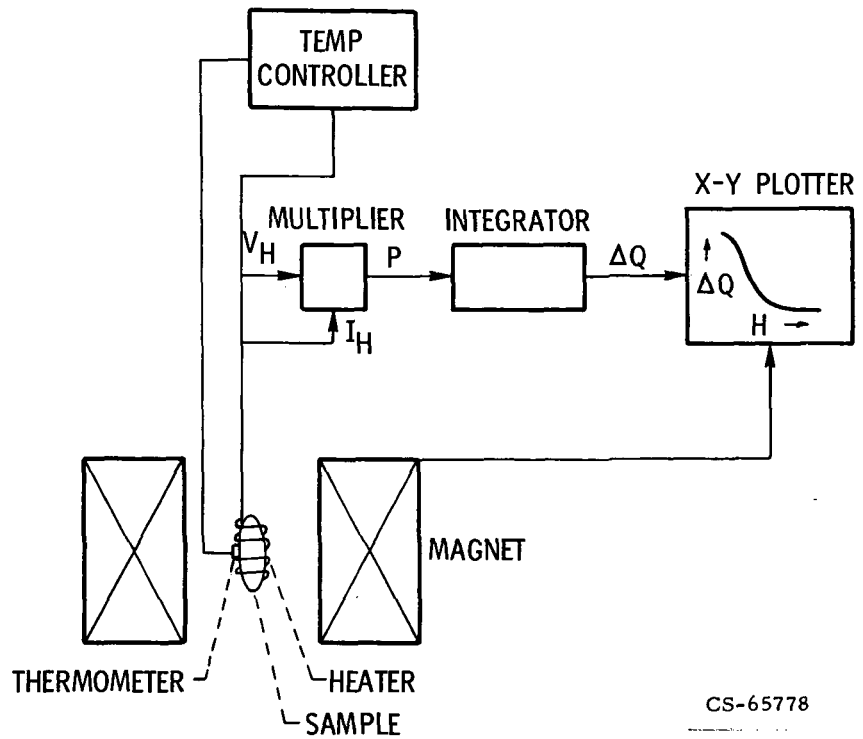
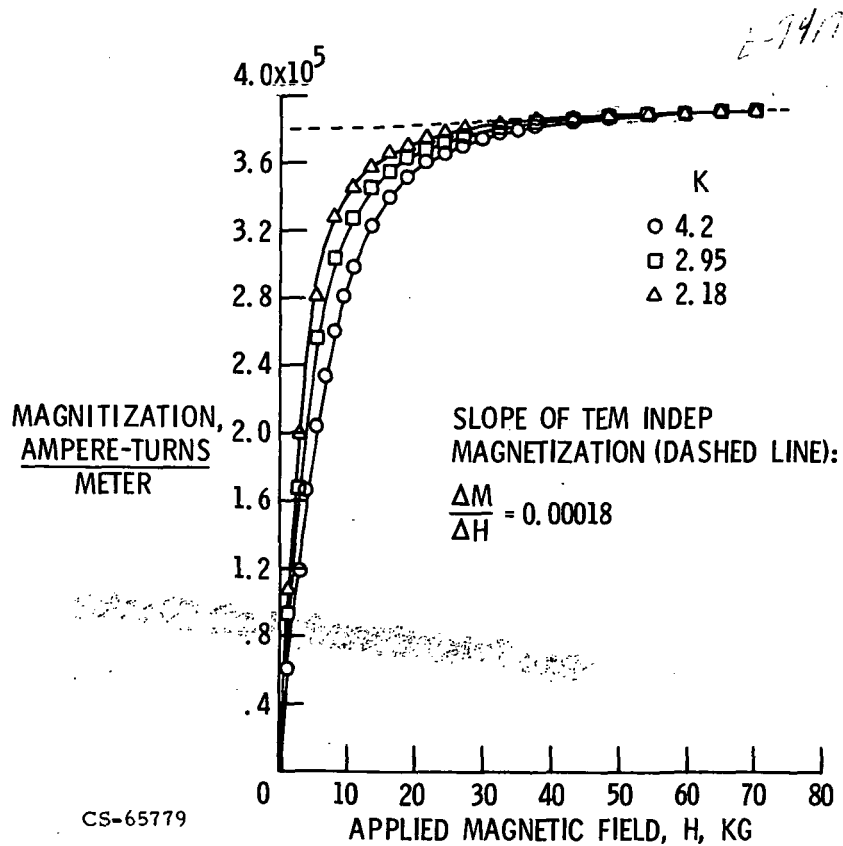Figure 3. – Schematic diagram of magnetic entropy measurement technique.

Figure 4. – Magnetization of $Dy_2Ti_2O_7$ as a function of applied magnetic field.
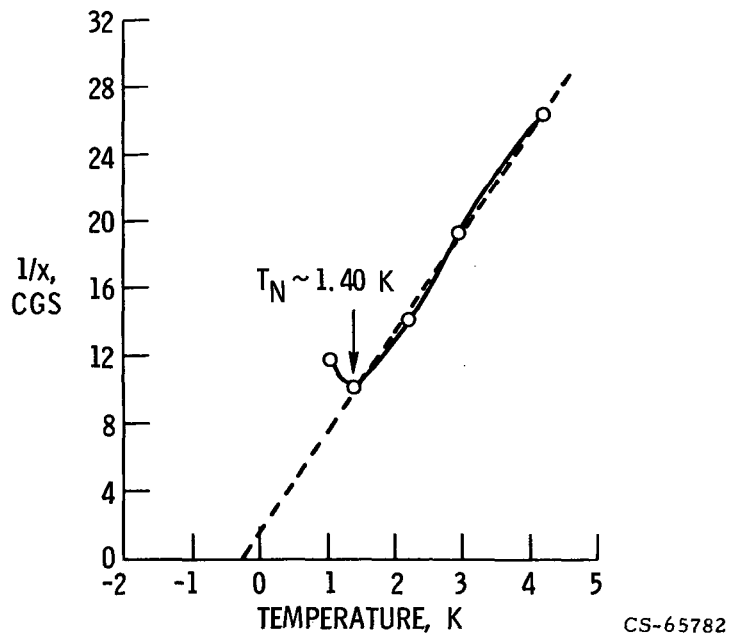
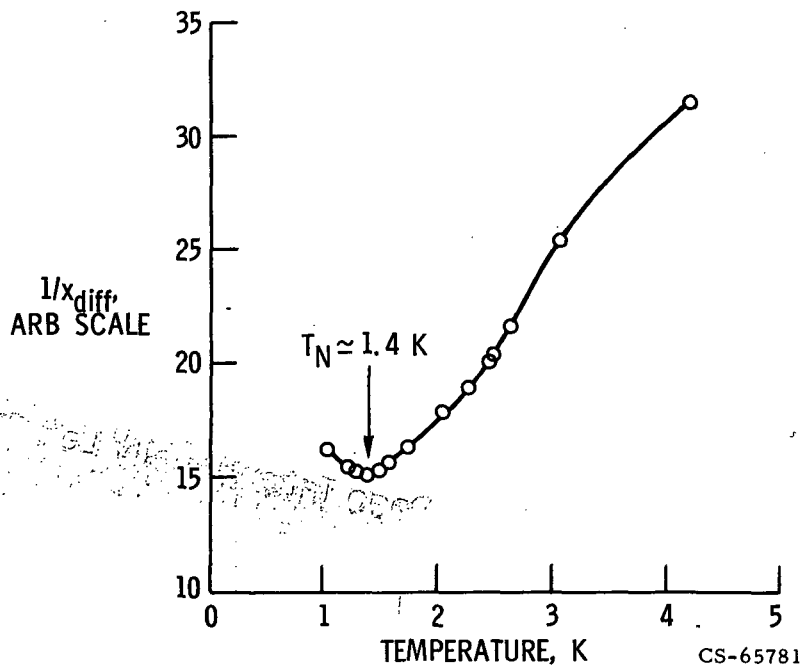Figure 5. - Reciprocal magnetic susceptibility of $Dy_2Ti_2O_7$.

Figure 6. - Reciprocal differential magnetic
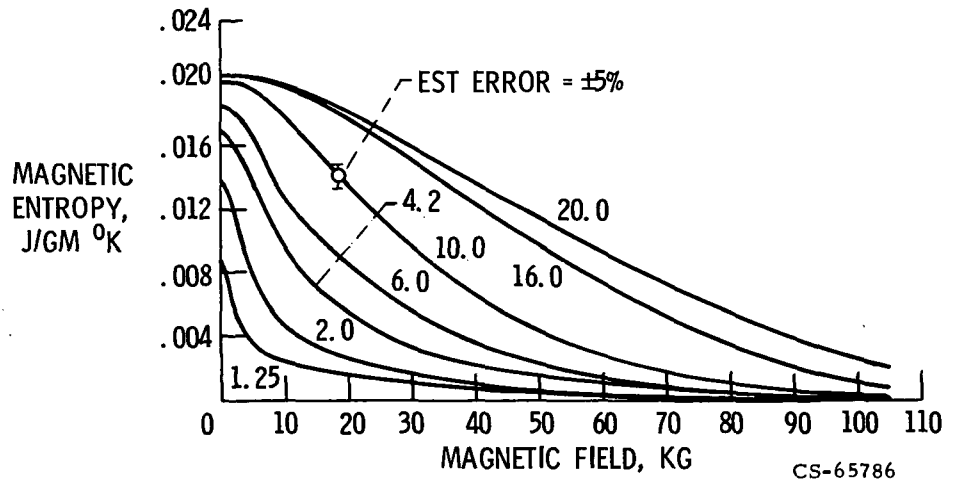susceptibility of $Dy_2Ti_2O_7$.

Figure 7. - Magnetic entropy of $Dy_2Ti_2O_7$ as a function of applied magnetic field.
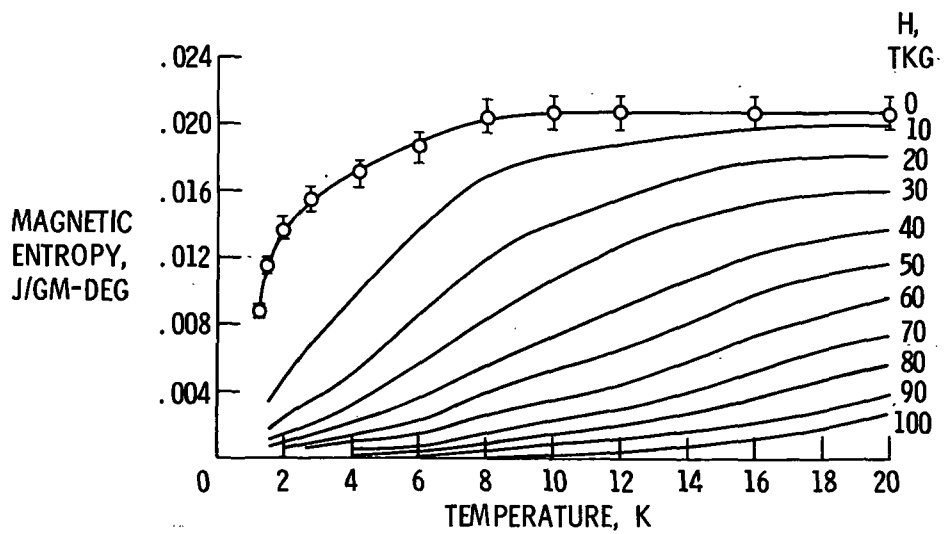

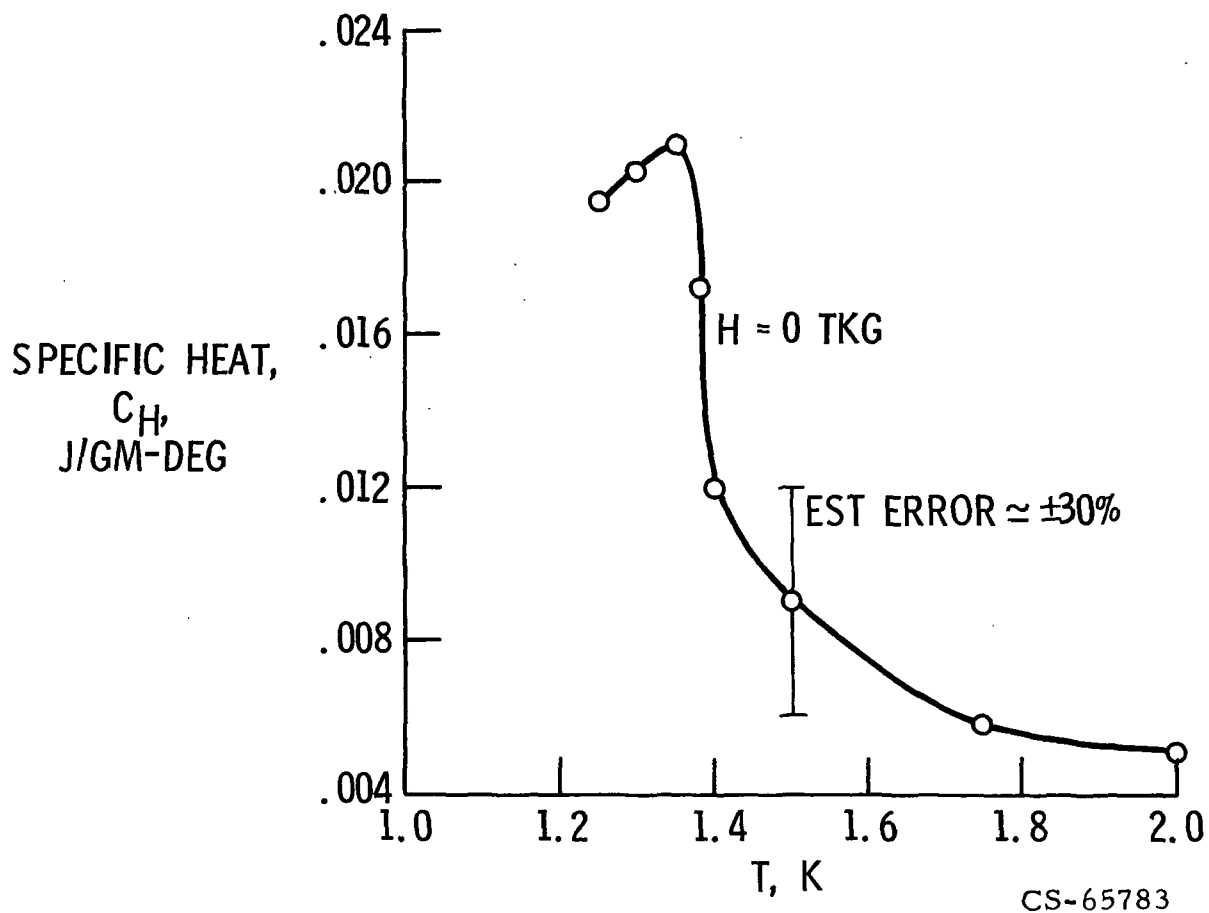Figure 8. - Magnetic entropy of $Dy_2Ti_2O_7$ as a function of temperature.

SPECIFIC HEAT,
C_H,
J/GM-DEG

.024

.020

.016

.012

.008

.004

1.0   1.2   1.4   1.6   1.8   2.0

T, K

H = 0 TKG

EST ERROR $\simeq \pm30\%$

CS-65783

Figure 9. – Magnetic specific heat of $Dy_2Ti_2O_7$
derived from zero-field magnetic entropy.